Orientation and Dynamics of Peptides in Membranes Calculated from 2H-NMR Data

ARTICLE *in* BIOPHYSICAL JOURNAL · MAY 2009

Impact Factor: 3.97 · DOI: 10.1016/j.bpj.2009.02.040 · Source: PubMed

4 AUTHORS, INCLUDING:

Santiago Esteban-Martín
Barcelona Supercomputing Center
31 PUBLICATIONS **603** CITATIONS
SEE PROFILE

Jesús Salgado
University of Valencia
95 PUBLICATIONS **1,726** CITATIONS
SEE PROFILE

Orientation and Dynamics of Peptides in Membranes Calculated from ^{2}H-NMR Data

Erik Strandberg,[†] Santi Esteban-Martín,[‡] Jesús Salgado,[‡§] and Anne S. Ulrich[¶*]

[†]Karlsruhe Institute of Technology, Institute for Biological Interfaces, Forschungszentrum Karlsruhe, 76021 Karlsruhe, Germany; [‡]Instituto de Ciencia Molecular, Universidad de Valencia, 46980 Paterna (Valencia), Spain; [§]Departamento de Bioquímica y Biología Molecular, Universidad de Valencia, 46100 Burjassot (Valencia), Spain; and [¶]Institute of Organic Chemistry, University of Karlsruhe, 76131 Karlsruhe, Germany

ABSTRACT Solid-state ^{2}H-NMR is routinely used to determine the alignment of membrane-bound peptides. Here we demonstrate that it can also provide a quantitative measure of the fluctuations around the distinct molecular axes. Using several dynamic models with increasing complexity, we reanalyzed published ^{2}H-NMR data on two representative α-helical peptides: 1), the amphiphilic antimicrobial peptide PGLa, which permeabilizes membranes by going from a monomeric surface-bound to a dimeric tilted state and finally inserting as an oligomeric pore; and 2), the hydrophobic WALP23, which is a typical transmembrane segment, although previous analysis had yielded helix tilt angles much smaller than expected from hydrophobic mismatch and molecular dynamics simulations. Their ^{2}H-NMR data were deconvoluted in terms of the two main helix orientation angles (representing the time-averaged peptide tilt and azimuthal rotation), as well as the amplitudes of fluctuation about the corresponding molecular axes (providing the dynamic picture). The mobility of PGLa is found to be moderate and to correlate well with the respective oligomeric states. WALP23 fluctuates more vigorously, now in better agreement with the molecular dynamics simulations and mismatch predictions. The analysis demonstrates that when ^{2}H-NMR data are fitted to extract peptide orientation angles, an explicit representation of the peptide rigid-body angular fluctuations should be included.

INTRODUCTION

The orientation of membrane-bound peptides in lipid bilayers can be routinely determined by solid-state NMR (SSNMR) (1,2). For a simple α-helix, this orientation is defined by the tilt angle of its long axis with respect to the membrane normal, plus an azimuthal angle giving the rotation of the helix around its axis. This alignment is typically calculated from a number of local orientational constraints acquired from ^{2}H- ^{19}F- or ^{15}N-labeled peptides (3–15). However, such analysis of the NMR data normally ignores, or oversimplifies, the molecular motions of the peptide, which are clearly nonnegligible in a fluid lipid bilayer. Other spectroscopic methods for estimating peptide orientation in membranes, such as oriented circular dichroism (16,17) or attenuated total reflection Fourier-transform infrared spectroscopy (18), are not able to provide this dynamic information either.

As relatively small molecules, peptides are expected to be highly mobile in liquid crystalline membranes. For instance, internal peptide-plane librations occur on the timescale of 10^{-9} s, whereas whole-body axial diffusion and off-axial reorientations may take place on the 10^{-8}–10^{-7} s and 10^{-6}–10^{-5} s timescales, respectively (19,20). Because these molecular motions are much faster than the SSNMR acquisition timescale of up to a second, peptide dynamics will lead to a partial averaging of the anisotropic NMR signals. The amplitudes of fluctuation can thus have a direct effect on the apparent peptide orientation angles, especially when these are calculated on the usual assumption of a simple static model. This problem was recently demonstrated by molecular dynamics (MD) simulations on the model peptides WLP23, KLP23, and WALP23 (21,22). The authors showed that large deviations can exist between the actual time-averaged helix tilt and rotation angles as deduced directly from the MD traces and the calculated values that were either evaluated indirectly from the simulated ^{2}H-NMR splittings or obtained directly by experiment. In fact, these and other MD studies (23,24) have systematically yielded much larger tilt angles of the peptides (30–40°) than determined from ^{2}H-NMR experiments of the same systems (4–10°).

It is therefore essential to account for motional averaging when calculating the peptide orientation from SSNMR data. However, so far, peptide mobility has been ignored or, at most, has been considered by introducing a fixed or adjustable order parameter S (3,5,7,8,10–12,14). Here, we present a detailed analysis of the influence of peptide dynamics on the interpretation of ^{2}H-NMR data, where the anisotropic fluctuations of the peptide motions of and around its helix axis are modeled explicitly. By reanalyzing the published ^{2}H-NMR data from several peptide/lipid systems, using a number of alternative models of increasing complexity to account for peptide mobility, we obtain what we believe is a new view of peptide dynamics in membranes. In an accompanying article (25) we do a similar analysis of the influence of dynamics on the interpretation of ^{15}N-NMR data from polarization inversion spin exchange at the magic angle (PISEMA) experiments.

Our systems of choice are the amphipathic antimicrobial peptide PGLa and the hydrophobic model peptide WALP23. Each of these has been selectively labeled with

Submitted October 21, 2008, and accepted for publication February 17, 2009.

*Correspondence: anne.ulrich@ibg.fzk.de

Editor: Marc Baldus.

0006-3495/09/04/3223/10 $2.00

doi: 10.1016/j.bpj.2009.02.040

Ala-d_3 in at least eight different positions, and ^{2}H quadrupolar splittings have been systematically collected in different model membranes and under different conditions (7,10–12). The selected examples thus represent the various orientations that are typically encountered for helical peptides in liquid crystalline membranes, as illustrated in Fig. 1, which should be of general interest for many other systems too. Specifically, we consider here the amphiphilic PGLa helix in DMPC, bound flat to the membrane surface in the so-called ''S-state'' as a monomer (Fig. 1 *A*), embedded in the bilayer in a tilted ''T-state'' as a putative dimer (Fig. 1 *B*), and immersed in the membrane in the ''I-state'' in an almost upright alignment (Fig. 1 *C*). Unlike PGLa, the fully hydrophobic WALP23 is always expected to assume a transmembrane alignment, e.g., in DMPC (Fig. 1 *D*), although in a DLPC bilayer, the mismatch in hydrophobic thickness is expected to induce a more significant tilting (Fig. 1 *E*) (3,7,26).

For each of these five cases we have calculated the best-fit helix tilt and azimuthal rotation angles by an rmsd analysis of the NMR data, using for these analyses several different dynamic models. We find that the inclusion of dynamics improves the quality of the fits, and the applicability versus complexity of the models is discussed in terms of the multiple-parameter fits. Obviously, the apparent deviations of the calculated structures depend primarily on the extent of motion, but more remarkably, the reliability of the analysis depends also very much on the actual orientation of the peptide. Altogether, the most appropriate model, which assumes explicit fluctuations of and around the helix axis, appears to be most realistic and allows for the first time, to our knowledge, to estimate the amplitudes of peptide whole-body motions in the membrane.

METHODS

Structural model for the conformation and orientation of membrane peptides

The peptides studied here are known to be α-helical in lipid environments from circular dichroism and NMR analysis (6,27–30) Hence, they are modeled as an ideal polyalanine helix, with the same backbone conformation for all residues (6,8). The geometric analysis of labeled alanines (GALA method) utilizes Ala-d_3 residues as selective labels (8,11), for which the orientation of the C_α–$C_\beta D_3$ vector is fixed by the backbone structure. This molecular geometry is described by a pair of angles, α and β. The first one is defined within the plane normal to the helix axis through the C_α atom, and it is the angle formed between the projection of the C_α–C_β bond onto that plane and a radial vector from the peptide axis to the C_α. In turn, β is the angle between the C_α–C_β bond and the helix axis. In an α-helical polyalanine model constructed using SYBYL (Tripos, St. Louis, MO) with backbone angles $\varphi = -58^\circ$ and $\psi = -47^\circ$ and a pitch between contiguous residues of $\gamma = 100^\circ$, the values of α and β are 53.2° and 121.1°, respectively (6). The definitions of the angles are shown in Fig. S1 in the Supporting Material.

The orientation of the peptide helix in the lipid membrane is defined by the tilt angle τ between the helix axis and the membrane normal and by the azimuthal rotation angle ρ about the helix axis (Fig. 2). The reference for the zero value of ρ can be set according to different conventions. Here, in all cases, we will use the same convention as in our publications on PGLa (5,8,10–12,27), for which $\rho = 0$ when the radial vector pointing through C_α of residue number 12 lies in a plane parallel to the membrane surface. However, whenever a different convention was used in previous experimental work, as for WALP23 peptides, to avoid confusion, we also state the ρ-values according to those original publications (3,7).

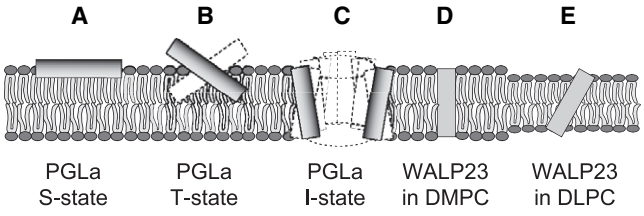

FIGURE 1 Representative orientational states of membrane-bound peptides in the different peptide-lipid systems studied. (*A*) Surface-aligned amphiphilic peptide (S-state), PGLa/DMPC 1:200. (*B*) Tilted dimer (T-state), PGLa/DMPC 1:50. (*C*) Membrane-inserted oligomer (I-state) in a putative pore, PGLa/MAG/DMPC/DMPG 1:1:75:25. (*D*) Transmembrane state of a monomeric hydrophobic peptide, WALP23/DMPC 1:100. (*E*) Mismatched transmembrane state of a monomeric hydrophobic peptide, WALP23/DLPC 1:100. In all panels the hydrophobicity of peptides and lipids is indicated by a gray scale, where the more polar parts are shaded darker.

Theoretical splittings in static and dynamic models

Calculations were performed on a PC using FORTRAN programs. The basic formula connecting the deuterium quadrupolar splittings to the structure and orientation of a helical peptide is (7)

$$\Delta\nu_q = \Delta\nu_q^0\, 1/2\left[3\cos^2\beta(\cos\tau - \sin\tau\cos\delta\,\tan\beta)^2 - 1\right], \quad (1)$$

where $\Delta\nu_q$ is the measured quadrupolar splitting, and $\Delta\nu_q^0$ is the maximum splitting that is related to the quadrupolar coupling constant e^2qQ/h. The angles τ (the helix tilt) and β are defined above, and δ is the local azimuthal rotation angle of the C-CD_3 bond vector of an Ala-d_3 residue, which in turn is related to the helix azimuthal rotation, ρ, by $\delta = \rho + \alpha + \theta$. Here, θ is the angle around the peptide axis between the reference residue (see definition above) and the CD_3-labeled Ala residue. For a regular helix $\theta = n\gamma$, with n being the number of residues between the reference and the labeled residue, and γ is defined above (7,10). Together with γ, the bond angles α and β define the rigid helical peptide conformation (see above and Fig. S1).

Equation 1 represents a static model that can be fit to a set of experimental ^{2}H-NMR splittings. To account for motional averaging in the most simplistic way, this expression can be multiplied by an order parameter $0 \le S \le 1$, which has the effect of scaling down all couplings (4,5,8,10–12). In a more advanced model of peptide dynamics, we can also describe the oscillatory fluctuations of the peptide around its helix axis by assuming a Gaussian distribution of ρ angles, centered at ρ_0, and with a standard deviation of σ_ρ (21);

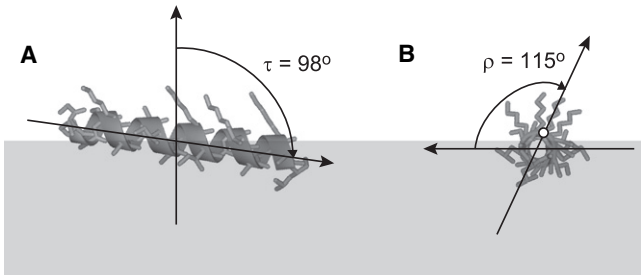

FIGURE 2 Definition of the helix tilt angle τ and its azimuthal rotation ρ, illustrated here for PGLa in the S-state (for details see text).

$$d(\rho) = N \exp\left[-(\rho_0 - \rho)^2 / \left(2\sigma_\rho^2\right)\right], \quad (2)$$

where N is a normalization constant, $N = (\sigma_\rho \sqrt{(2\pi)})^{-1}$. The splittings calculated for all different ρ-angles are weighted by the probability distribution and integrated to give the averaged effective splitting $\Delta\nu_q$. An analogous calculation can be done to account for a distribution of τ-angles, corresponding to a wagging of the helix axis, using a Gaussian distribution centered at τ_0 and with a width of σ_τ. Ultimately, both τ- and ρ-fluctuations can be considered simultaneously by using Gaussian distributions of the two angles and performing a two-dimensional integration.

When analyzing the ^{2}H-NMR data using any of these models, the calculated quadrupole splittings for each CD_3-labeled position are compared with the experimental value of the splitting, and the root mean-square deviation (rmsd) is minimized using a multidimensional grid search of the free parameters. Because the signs of the experimental splittings are unknown, the fits and rmsd calculations are performed using the absolute values of the calculated splittings.

RESULTS AND DISCUSSION

Peptide-lipid systems used in the study

To test and compare the various dynamic models, they are applied here to several different peptide/lipid systems covering a wide range of orientations, oligomerization, and binding modes. Each case chosen has been studied in depth by solid-state ^{2}H-NMR using peptides labeled with Ala-d_3 in at least eight different positions, which gives sufficiently large data sets to allow reliable fits with up to five free parameters. All the data have been published previously, and for experimental details, the reader should consult the original articles (7,10,12). See also comments on the data in the Supporting Material.

The antimicrobial peptide PGLa (GMASKAGAIAG KIAKVALKAL-amide) forms an amphipathic α-helix in lipid environments. For a peptide/lipid molar ratio (P/L) of 1:200, the helix was found to lie almost parallel to the membrane surface (8,10). This so-called ''S-state'' (see Fig. 1 *A*) is proposed to be the preferred state for most amphipathic peptides at low concentration. At a higher concentration of PGLa in DMPC (P/L=1:50), an oblique tilt of the helix was observed (see Fig. 1 *B*), and this so-called ''T-state'' has been proposed to consist of peptide dimers (8,10). A similar T-state has been found for other amphipathic peptides and might be common (14,28). A third orientational state was detected for PGLa in 1:1 mixtures with magainin-2 (MAG), another antimicrobial peptide found in the same frog skin, which is known to have a synergistic effect on PGLa (33). In the PGLa/MAG system, PGLa was found to have a small tilt angle (12). This transmembrane ''I-state'' indicates the existence of a transmembrane pore (see Fig. 1 *C*). Such a pore has been suggested to be the physical cause of bacterial death, and it is biologically relevant to study this state for antimicrobial peptides in general (17,29,30).

Transmembrane model peptides were first introduced by Davis (31). As a representative case, we chose here WALP23 (acetyl-GWW(LA)$_8$LWWA-amide) from the WALP family of peptides, which has been studied systematically by Killian et al. (for a recent review see Killian and Nyholm (32)). The orientation of the peptide was determined with ^{2}H-NMR in different lipid systems to examine the effect of hydrophobic mismatch (7). We here use data from WALP23 in DMPC (almost matching, see Fig. 1 *D*), and in DLPC (where the peptide is too long and is expected to tilt, see Fig. 1 *E*). The calculated tilt angles increased slightly with decreasing membrane thickness, but they covered only a small range (5° to 8° for WALP23, from thicker toward thinner membranes), which appears insufficient to provide much mismatch relief (7). Moreover, several MD simulations performed on WALP and related peptides in different lipid systems have generally shown much larger tilt angles (21–23, 27,33–37). It is therefore interesting to understand the discrepancy between the NMR and MD analysis, which has been recently attributed to the question of whether and how peptide dynamics is considered in the NMR analysis (21,22).

Evaluation of alternative models of peptide orientation and dynamics

Model 1: Static splitting (fit of τ and ρ)

In the simplest approach, the experimental data are fitted to Eq. 1 with the tilt angle τ and the azimuthal rotation ρ as the only free parameters. The maximum quadrupolar splitting $\Delta\nu_q^0$ is reported in the literature with a value of $Q_{cc} =$ 168 kHz for a completely immobile aliphatic ^{2}H-C bond, which corresponds to a maximum splitting for a rotating CD_3-group of $\Delta\nu_q^0 = 84$ kHz (38). We use this value in Model 1 to evaluate the peptide orientation (see below) under the assumption of completely static conditions.

Model 2: Scaled splitting (fit of τ and ρ)

In dry peptide powders at room temperature, we experimentally obtain a maximum splitting of only ~74 kHz (P. Tremouilhac, E. Strandberg, P. Wadhwani, and A. S. Ulrich, unpublished results for Ala-d_3-labeled PGLa), which is indicative of some intrinsic internal motions of the peptide. Similar values are also observed for other Ala-d_3-labeled peptides. In Model 2 we therefore use this value of $\Delta\nu_q^0$=74 kHz instead of the static splitting of Model 1, as the membrane-bound peptides are likely to be at least as mobile as in a dry powder. This choice is equivalent to introducing a scaling factor (order parameter) $S^i = 0.88$, accounting for some intrinsic internal mobility of the peptide that would reduce the maximum value of the splitting down to the dry-powder value (3,7).

The best-fit values of τ and ρ are listed in Table 1 for the different peptide-lipid systems, using either $\Delta\nu_q^0 = 84$ kHz (Model 1) or $\Delta\nu_q^0 = 74$ kHz (Model 2). Generally, for a given peptide/lipid system, it is seen that the values of τ and ρ are almost the same, irrespective of the $\Delta\nu_q^0$ value (except for ρ in the S-state of PGLa). Yet, Model 2 gives better solutions with lower rmsd values compared to Model 1. This finding confirms that the peptides experience some motional averaging, which can be advantageously accounted for by using

TABLE 1 Best-fit parameters using Models 1, 2, and 3

	Model 1 $\Delta\nu_q^0 = 84$ kHz ($S^i = 1$)			Model 2 $\Delta\nu_q^0 = 74$ kHz ($S^i = 0.88$)			Model 3 variable S ($0 \leq S \leq 1$)			
Peptide/lipid system	τ/°	ρ/°	rmsd/kHz	τ/°	ρ/°	rmsd /kHz	τ/°	ρ/°	S	rmsd /kHz
PGLa in the S-state*	97	34	8.0	97	117	5.7	98	115	0.70	2.1
PGLa in the T-state*	121	113	8.0	124	112	3.9	126	111	0.78	1.2
PGLa in the I-state†	162	97	2.2	158	98	1.2	157	98	0.84	1.1
WALP23 in DMPC‡	4	293 (167)	2.2	6	300 (160)	1.5	7	302 (158)	0.72	1.0
WALP23 in DLPC‡	3	266 (194)	3.4	7	285 (175)	4.0	15	318 (142)	0.51	2.3

*From Strandberg et al. (10).
†From Tremouilhac et al. (12).
‡From Strandberg et al. (7). The ρ-values calculated according to the conventions of the original WALP23 publication are given in parentheses to allow comparison with the previous analysis.

a scaled quadrupolar coupling constant, as previously used (3,7). Nevertheless, the errors are still rather large in some cases (intrinsic experimental errors are ~1 kHz); hence even Model 2 with a scaled splitting does not appear to describe these systems appropriately.

Model 3: Variable S (fit of τ, ρ, and S)

We now consider additional peptide dynamics, other than that included via the initial $S^i = 0.88$. For clarity, we introduce a second order parameter, S^r, to account for the motions not captured by S^i, such as additional internal vibrations and especially partial rotations and wobbling of the whole molecule, which are expected to occur in the bilayer environment. The global order parameter S, which corresponds to the total dynamic averaging, is a product of the two order parameters ($S = S^i \times S^r$, $0 \leq S \leq 1$) and will be used as a fitting parameter together with τ and ρ. The adjustable order parameter S acts as a scaling factor to reduce the nominal $\Delta\nu_q^0 = 84$ kHz coupling constant. Thus, Models 1 and 2 are special cases of the more general Model 3. This variable S model has been introduced and successfully used by our group as a rough measure of dynamics in the analysis of PGLa and many other peptides (2,4,8,10–12,14,39).

Table 1 contains the best-fit values of τ, ρ, and S for the different peptide-lipid systems. The variable S model produces better fits than the static models used above, with all rmsd values between 1 kHz and 2 kHz. The biggest improvements in rmsd within each peptide system are seen for the small S values, namely for PGLa in the S-state and for WALP23. The model dependence is not so pronounced for PGLa in the I-state, which has a high S value and is the least mobile system. It is also seen that the angles τ and ρ are similar to those obtained with Model 2 except for WALP23 in DLPC, which has a particularly small S (and for which τ goes from 7° to 15°). The data are often analyzed by rmsd plots and helical wave plots, as described in the Supporting Material.

Model 4: Explicit azimuthal fluctuations (fitted τ, ρ_0, and σ_ρ)

In the next models we still perform a three-parameter fit, but instead of using a variable order parameter S, we describe the peptide dynamics in a more explicit manner. First, let us consider specific whole-body peptide dynamics, which consists of rotational oscillations around the helix axis. These fluctuations can be modeled with a Gaussian (normal) frequency distribution of the ρ-angle, which assigns maximum probability to the mean value ρ_0 and is characterized by a certain standard deviation of σ_ρ (there is 68% probability that ρ is within the interval $\rho_0 \pm \sigma_\rho$). The choice of a Gaussian distribution is motivated mainly by our previous MD simulations (21). A uniform distribution, with equal probability over a specified range of angles, although easy to implement, would disagree with the MD results (21,22,35). On the other hand, more complex distributions, such as a bimodal distribution centered on two preferred angles, would introduce additional parameters and be much too complex to allow finding a solution with the amount of data usually available. We assume that the fluctuations are fast compared to the NMR timescale, so that the distribution will lead to an averaging of the quadrupolar splittings in an anisotropic way, thus modifying the shape of the helical wave curve. We use the dry powder value $\Delta\nu_q^0 = 74$ kHz from Model 2 as the quadrupolar splitting constant, assuming that the internal dynamics in the peptide powder will be present to a similar extent for peptides in a hydrated membrane ($S^i = 0.88$).

Fits were systematically performed for the peptide/lipid systems over a range of σ_ρ-values. The results are presented in Fig. 3, where the best-fit values of τ, ρ_0, and the corresponding rmsd are shown as a function of the standard deviation σ_ρ. The best-fit values for the different systems are given in Table 2. The results for PGLa in the S-state are presented in Fig. 3 *A*. It is seen that there is a clear minimum in the rmsd curve at $\sigma_\rho = 19°$. However, for σ_ρ in the range of up to 35° the best-fit τ and ρ_0 values are almost constant and within 2° of the best values of Model 3 (variable S). We conclude that rotation about the helix axis with a distribution width σ_ρ of 19° can give a good fit and that τ and ρ_0 are quite well defined for this surface-bound monomeric peptide. For the putative PGLa dimers in the T-state, we observe a similar behavior (Fig. 3 *B*), with a best fit again for $\sigma_\rho = 20°$, and corresponding τ and ρ_0 very similar compared to those from Model 3, although with slightly larger rmsd (see Table 2).

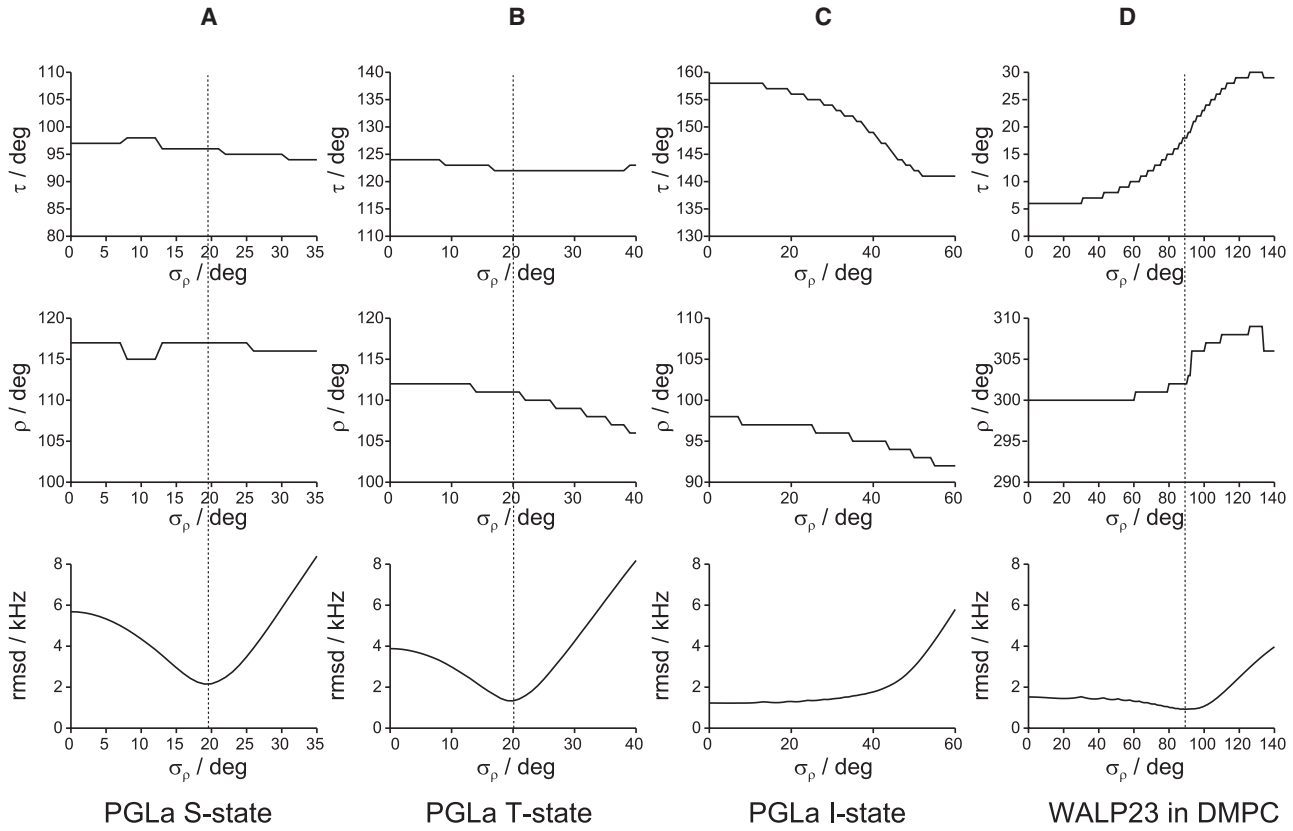

FIGURE 3 Finding the best-fit value for the azimuthal fluctuation σ_ρ and visualization of the corresponding variations in τ and ρ_0 (Model 4). The dashed line in each column indicates the best fit. (*A*) PGLa in the S-state, giving $\sigma_\rho = 19°$, $\rho_0 = 117°$. (*B*) PGLa in the T-state, giving $\sigma_\rho = 20°$, $\rho_0 = 111°$. (*C*) PGLa in the I-state, giving σ_ρ in the range of 0–25°, $\rho_0 = 97°$. (*D*) WALP23 in DMPC, giving $\sigma_\rho = 89°$, $\rho_0 = 302°$. WALP23 in DLPC has a similar appearance as in DMPC (data not shown).

For the oligomeric assembly of PGLa in the transmembrane I-state, the situation is quite different (Fig. 3 *C*). We see no clear minimum, and for σ_ρ in the range of 0° to 25° the rmsd remains very low, between 1.2 and 1.3 kHz. However, the tilt angle is here more sensitive to the ρ-distribution, going from 158° down to 145° with increasing σ_ρ (from 0° to 40°), whereas the average azimuthal rotation ρ_0 changes only by a few degrees. It seems in this case that including averaging motions around the helix axis does not improve the fits but introduces ambiguity of the tilt because there are many different combinations of τ and σ_ρ giving the same, or very similar, rmsd.

The most striking effect is seen for the transmembrane WALP peptides. For WALP23 in DMPC (Fig. 3 *D*), the best fit is obtained for a very broad distribution of ρ ($\sigma_\rho = 89°$). Clearly, there is a considerable probability for all azimuthal angles, meaning that the peptide can exhibit virtually complete rotation about its helix axis, although still with

TABLE 2 Best-fit parameters using Gaussian distributions of either ρ (Model 4) or τ (Model 5) or both simultaneously (Model 6), in all cases with $\Delta\nu_q^0 = 74$ kHz ($S^i = 0.88$)

	Model 4				Model 5				Model 6				
Peptide/lipid system	τ/°	ρ_0/°	σ_ρ/°	rmsd /kHz	τ_0/°	σ_τ/°	ρ/°	rmsd /kHz	τ_0/°	σ_τ/°	ρ_0/°	σ_ρ/°	rmsd/kHz
PGLa in the S-state*	96	117	19	2.2	100	26	115	2.3	98	17	115	15	2.0
PGLa in the T-state*	122	111	20	1.3	129	16	112	1.4	125	11	111	15	1.2
PGLa in the I-state†	157	97	1-25	1.2	157	8	99	1.1	155	8	98	20	1.1
WALP23 in DMPC‡	18	302 (158)	89	0.9	6	8	299 (161)	1.4	14	15	302 (158)	71	0.9
WALP23 in DLPC‡	34	317 (143)	91	2.3	8	15	285 (175)	3.6	29	26	317 (143)	66	2.2

*From Strandberg et al. (10).
†From Tremouilhac et al. (12).
‡From Strandberg et al. (7). The ρ-values calculated according to the conventions of the original WALP23 publication are given in parentheses to allow comparison with the previous analysis.

a most probable azimuthal angle that is almost the same for all σ_ρ-values (ρ_0 varies $<10^\circ$ when σ_ρ changes from 0° to 140°). However, and most notably, the calculated tilt angle increases with σ_ρ, from 6° for $\sigma_\rho = 0^\circ$ to 19° at $\sigma_\rho = 89^\circ$. For WALP in DLPC, a similar behavior is obtained (result shown in Table 2 but not in Fig. 3).

Fig. S3 visualizes the effect of rotation around the helix axis on the helical waves, and illustrates why this type of dynamics has a larger effect on the fit of peptides in a transmembrane orientation.

Model 5: Explicit wagging fluctuations (fit of τ_0, σ_τ, and ρ)

As an alternative to Model 4, we may also consider a Gaussian distribution of tilt angles for a helix with its azimuthal rotation fixed. Such a peptide can waggle in the membrane around a most probable, averaged tilt, τ_0, according to a normal probability distribution of width σ_τ. This motion will also lead to an averaging of splittings and will modify the helical wave curves in a different way compared to the ρ distribution Model 4. Fits were performed for all the peptide/lipid systems using a range of values of σ_τ (with $\Delta\nu_q^0 = 74$ kHz, see above), and the results are presented in Table 2. For PGLa, almost the same orientation is found as for Models 3 and 4. For PGLa in the I-state, no clear minimum was found. For WALP23, very small tilt angles are found, and the rmsd is larger than that for Models 3 and 4. In this case, the fit is more similar to that of Model 2. A detailed analysis of Model 5 is given in the Supporting Material, where fits are also shown in Fig. S6. The small allowed σ_τ-values for the transmembrane (small tilt) peptides can be understood from the effect of σ_τ on helical curves. This is shown in Fig. S5.

Model 6: Explicit τ- and ρ-fluctuations (fit of τ_0, σ_τ, ρ_0, and σ_ρ)

It is instructive now to introduce another free parameter in the fit, to be able to consider two separate distributions of both τ and ρ. We will treat their respective contributions individually, even though these two types of motion are of course present simultaneously and may partly compensate each another. Thus, in Model 6, we assume that the τ- and ρ-fluctuations are independent, and we use $\Delta\nu_q^0 = 74$ kHz ($S^i = 0.88$) to account for nonspecific internal motions.

A two-dimensional map of (σ_τ, σ_ρ) pairs taken from the best fits is shown in Fig. 4 *A* for the case of PGLa in the S-state, with color-coded rmsd values. Pairs with similar rmsd cluster together giving banana-shaped regions, indicating that the effects of σ_τ and σ_ρ are indeed not completely independent from each other. The preferred region has rmsd < 2.5 kHz, and a shallow minimum is found for $\sigma_\tau = 17^\circ$, $\sigma_\rho = 15^\circ$. Both of these values are smaller than those found using individual distributions, and they correspond to the best-fit case of $\tau_0 = 98^\circ$ and $\rho_0 = 115^\circ$. All these values, together with other results derived from Model 6, are summarized in Table 2. We note that τ_0 and ρ_0 represent the same orientation as the one found above with the variable S (Model 3) but with a slightly lower rmsd (2.0 kHz). It is also worth correlating the (σ_τ, σ_ρ) plot with a (τ_0, ρ_0) plot with pairs of best-fit orientation angles mapped to their corresponding color-coded rmsd (Fig. 4 *D*). In this case, we see that the banana-shaped region with rmsd < 2.5 kHz in Fig. 4 *A* corresponds to a very small area in the (τ_0, ρ_0) plot, and only a small range of the angles map to rmsd < 5 kHz.

An analogous analysis for PGLa in the T-state gives a similar picture (Fig. 4, *B* and *E*), where the preferred region

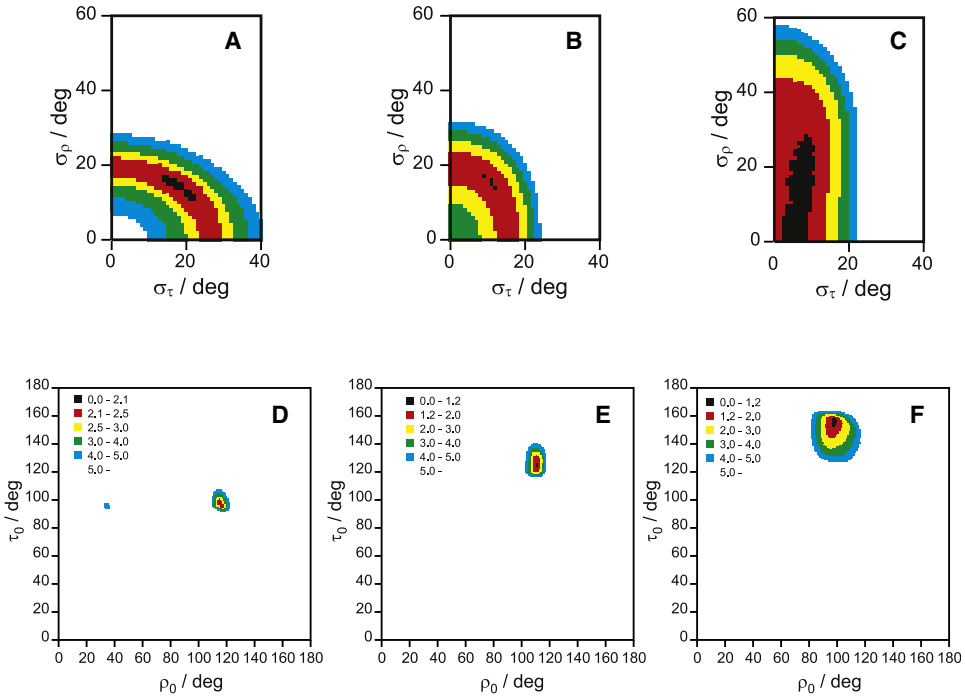

FIGURE 4 Plot of fitting the ^{2}H-NMR data as a function of (σ_τ, σ_ρ) for (*A*) PGLa in the S-state, (*B*) PGLa in the T-state, (*C*) PGLa in the I-state; and as a function of (τ_0, ρ_0) for (*D*) PGLa in the S-state; (*E*) PGLa in the T-state; and (*F*) PGLa in the I-state. The rmsd values for each point in the grid-search are indicated by a color code, with the same scale for the (σ_τ, σ_ρ) and (τ_0, ρ_0) plots of the same system.

(rmsd $<$ 2.0 kHz) is now shaped as an arc, and there is a minimum for $\sigma_\tau = 11°$ and $\sigma_\rho = 15°$ (not far from the values of the S-state). Such a minimum corresponds to $\tau_0 = 125°$ and $\rho_0 = 111°$, which is also very close to the values found above for a variable S (Model 3), with the same rmsd. In the (τ_0, ρ_0) plot, we see again a well-defined minimum, with a somewhat larger good-fit area compared to PGLa in the S-state.

The corresponding (σ_τ, σ_ρ) plot for PGLa in the I-state (Fig. 4 *C*) shows an allowed region that is much larger along the σ_ρ dimension. It is seen from the plot that for $\sigma_\tau = 0°$, a large range of σ_ρ-values give similar rmsd values, which explains why no clear minimum was found for Model 4 in this case (see Fig. S6 *C*). The best-fit area has a rather narrow range of σ_τ-values but a wide range of σ_ρ from 0° to 30°, with a tentative minimum at $\sigma_\tau = 8°$, $\sigma_\rho = 20°$, which is clearly different from that of the S- or T-states of PGLa. The angular values corresponding to this point ($\tau_0 = 155°$ and $\rho_0 = 98°$) compare well with the best fit from the variable S (Model 3), with the same rmsd. The (τ_0, ρ_0) plot (Fig. 4 *F*) has a unique minimum close to these values, but the region with an rmsd $<$ 5.0 kHz is much larger than that for PGLa in the S- or T-state. This means that the peptide orientation can be less well defined in the I-state, but it is still possible to pinpoint its alignment in terms of τ_0 and ρ_0 within ~±5° accuracy.

All PGLa systems have revealed well-defined distributions of τ and ρ that fit the experimental ^{2}H quadrupolar splittings very well. In all these cases, the best-fit rmsd is the same or slightly better compared to the analysis using the variable S (Model 3), and the tilt and azimuthal angles are virtually identical to the previously reported values based on that model. However, the newly introduced model of explicit whole-body fluctuations provides additional dynamic information on the respective amplitudes of wagging and azimuthal fluctuations, assuming ideal Gaussian distributions.

For WALP23 the emerging picture is rather different, presumably because this peptide is much more mobile than PGLa (see below). For WALP23 in DMPC, the region of the (σ_τ, σ_ρ) plot where rmsd $<$ 2 kHz is much wider, especially along the σ_ρ dimension, as illustrated in Fig. 5 *A*. There is a shallow minimum around $\sigma_\tau = 15°$ and $\sigma_\rho = 71°$, but the uncertainty in the fluctuation parameters is much larger than those for any of the PGLa cases described above. Clearly, the uniformly hydrophobic transmembrane peptide undergoes more extensive azimuthal fluctuations around its helix axis than the amphiphilic PGLa, although the fluctuations in the tilt angle are of comparable size. The best-fit orientation is for $\tau_0 = 14°$ and $\rho_0 = 302°$, and quite a large area in the (τ_0, ρ_0) plot corresponds to rmsd $<$ 2.0 kHz (Fig. 5 *C*). This solution corresponds to the same azimuthal angle but a considerably larger helix tilt compared to the analysis above using the variable S model (Model 3 with $\tau = 7°$). The calculated helix tilt is, in fact, very much larger than the previously reported angle (3,7). The previous analysis had been based on a model similar to our Model 2 above (see Table 1).

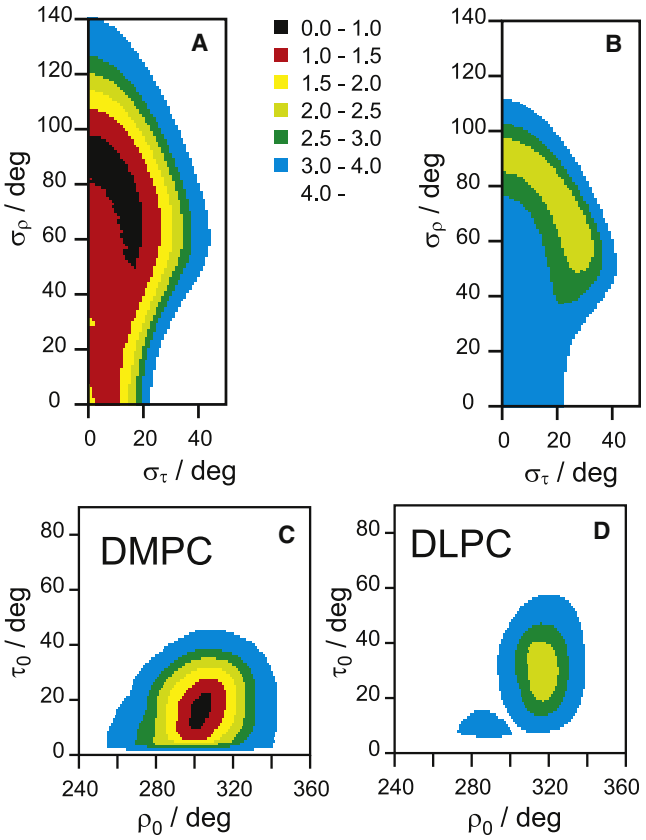

FIGURE 5 Plot of fitting the ^{2}H-NMR data as a function of (σ_τ, σ_ρ) for (*A*) WALP23 in DMPC, (*B*) WALP23 in DLPC; and as a function of (τ_0, ρ_0) for (*C*) WALP23 in DMPC, and (*D*) WALP23 in DLPC. The rmsd value for each point in the grid search is indicated by a color code, with the same scale in all graphs.

The divergence in τ_0 is even more pronounced when WALP23 is embedded in DLPC with shorter acyl chains, as seen in Fig. 5, *B* and *D* (see also Table 2). The best-fit helix tilt assuming the new dynamic model is $\tau_0 = 29°$, compared to $\tau = 15°$ for the variable S (Model 3), or $\tau = 7°$ (Model 2) or 3°, for the static Model 1. Thus, the previously examined hydrophobic mismatch effect for these types of WALP peptides, which was found to be unexpectedly small, has now become much clearer from our dynamic analysis, which supports more recent interpretations (21,22).

If we assume no intrinsic motion of the peptides ($S^i = 1$), the explicit dynamic models give, as could be expected, wider distributions of angles but have almost no effect on the orientation. Details are given in Table S1 and Table S2. For a discussion of combining distributions of τ and/or ρ angles with a variable S, see the Supporting Material.

We thus propose that Model 6 is most appropriate to extract the best-fit values or at least the feasible ranges of ρ_0 and τ_0 from the ^{2}H-NMR data, provided that a sufficient number of ^{2}H splittings is available, such as the eight values used here. Additionally, this dynamic analysis can give a good estimate of the amplitudes of peptide whole-body motions in the membrane, i.e., the azimuthal fluctuations

represented by σ_ρ and the fluctuations of the helix tilt represented by σ_τ. The results for PGLa and WALP23 using Model 6 are summarized in Table 2, where ρ_0 and τ_0 describe the classical alignment of the peptides, and σ_ρ and σ_τ may be regarded as describing their dynamic behavior. We see that the change in tilt angle τ_0 of PGLa in realigning from the monomeric S-state to the dimeric T-state and into the oligomeric I-state is accompanied by a decrease in the amplitude of wagging fluctuations. This trend of σ_τ going from 17° to 11° to 8° is in very good agreement with the proposed stepwise oligomerization of PGLa and the ensuing decrease in mobility (note that the values of ρ_0 and σ_ρ, connected to the amphiphilic character of the peptide, remain rather unaffected). It is also instructive to compare the mobility of PGLa in the I-state with that of WALP23 in DLPC, as both transmembrane helices have a very similar tilt angle τ_0 of 25° (τ = 155° and ρ = 98° is equivalent to τ = 25° and ρ = 278°, see Fig. S2) (PGLa) or 29° (WALP23). Yet, PGLa undergoes only moderate fluctuations with $\sigma_\tau = 8°$ and $\sigma_\rho = 20°$, whereas WALP23 is vigorously mobile with $\sigma_\tau = 26°$ and $\sigma_\rho = 66°$. These dramatic differences can certainly be attributed to the respective oligomeric and monomeric states of these two peptides. Finally, the effect of bilayer mismatch is nicely illustrated by the comparison of WALP23 in DMPC and DLPC. The helix is more upright in DMPC ($\tau_0 = 14°$) compared to the thinner DLPC bilayer ($\tau_0 = 29°$).

Choice of model for the ^{2}H-NMR data analysis

As seen above for the examples of PGLa and WALP23, using different dynamic models can give distinctly different results for the calculated peptide alignment. These values are summarized in Table 3, allowing us to compare the trends in τ_0, ρ_0, and rmsd for Models 1 to 6. It is seen that the ρ_0 values are hardly affected by whichever model is used (except for WALP23 in DLPC), so one does not need to worry about these. The rmsd values are seen to decrease significantly on introduction of, first, the fixed scaling factor $S^i = 0.88$ (Model 2) and then the variable order parameter (Model 3). Application of the fluctuation model around a single peptide axis (Model 4 shown here has better rmsd than Model 5) gives slightly worse rmsd values compared to Model 3, although the same number of free parameters are being fitted. Therefore, we conclude that Model 3 with a variable S should be generally preferable to Model 4 in cases where only a limited number of ^{2}H-NMR data are available (i.e., when Model 6 cannot be applied).

Attention must be paid to the tilt angle τ, as this value is found to depend most critically on the type of dynamic model applied. In the case of PGLa, which exhibits only moderate mobility in any of its three alignment states, the model dependence is not so pronounced. However, in the case of the vigorously mobile WALP23, the observed increase of τ on introduction of better dynamic models suggests that the helix tilt angle gets systematically underestimated when dynamics is not taken into account properly (21,22). The deviations can be up to one order of magnitude when the completely inappropriate static Model 1 is used (giving τ of 3° for WALP23 in DLPC, as opposed to 29° using Model 6), and they are still a factor of 2 when the reasonable Model 3 with a variable S is applied (giving τ of 15° for WALP23 in DLPC as opposed to 29°, or 7° as opposed to 14° in DMPC).

Apart from dynamics, the assumed conformational model also has an influence on the analysis. Using a canonical α-helix in our previous ^{19}F- and ^{2}H-NMR studies of amphipathic membrane-bound peptides has resulted in good fits to the data (4,5,8,10–12,14). The hydrophobic transmembrane

TABLE 3 Comparison of dynamic models

		Dynamic model				
Peptide system		Model 1 ($S = 1$)	Model 2 ($S = 0.88$)	Model 3 ($0 \leq S \leq 1$)	Model 4 (Variable ρ)	Model 6 (Variable τ, ρ)
PGLa in the S-state	Tilt τ (°)*	97	97	98	96	98
	Rotation ρ (°)*	34	117	115	117	115
	Rmsd (kHz)	8.0	5.7	2.1	2.2	2.0
PGLa in the T-state	Tilt τ (°)*	121	124	126	122	125
	Rotation ρ (°)*	113	112	111	111	111
	Rmsd (kHz)	8.0	3.9	1.2	1.3	1.2
PGLa in the I-state	Tilt τ (°)*	162	158	157	157	155
	Rotation ρ (°)*	97	98	98	98	98
	Rmsd (kHz)	2.2	1.2	1.1	1.2	1.1
WALP23 in DMPC	Tilt τ (°)*	4	6	7	18	14
	Rotation ρ (°)*	293	300	302	302	302
	Rmsd (kHz)	2.2	1.5	1.0	0.9	0.9
WALP23 in DLPC	Tilt τ (°)*	3	7	15	34	29
	Rotation ρ (°)*	266	285	318	317	317
	Rmsd (kHz)	3.4	4.0	2.3	2.3	2.2

*For cases of variable tilt and rotation angles, the given values correspond to means of Gaussian distributions.

helices, too, have been found to be highly uniform in PISEMA studies (40–42). Especially for the latter ones, the implicit assumption of a straight α-helix is expected to be valid, i.e., in the center of the hydrophobic core where all the Ala-d_3 labels are placed in the case of WALP23.

Nevertheless, it is useful to consider the possible impact of conformational deviations from this simplified input structure. One approach is to examine the rmsd values that remain in the best fits of the different systems studied. For example, PGLa in the S-state and WALP23 in DLPC show systematically worse rmsd values for all of the tested models, Models 1–6 (irrespective of any dynamics considered). This observation suggests that these relatively large residual errors may be at least in part caused by the actual conformation of the peptides.

CONCLUSIONS

We have investigated the influence of peptide mobility on the determination of molecular alignment from ^{2}H-NMR data, by evaluating different dynamic models of increasing complexity. For two representative peptides PGLa and WALP23 in various alignment states, this comprehensive analysis shows that good fits cannot be obtained unless some degree of dynamic averaging is included in the model.

The explicit dynamic analysis in terms of τ- and ρ-fluctuations (Model 6) shows that the amphipathic peptide PGLa undergoes moderate dynamics in liquid crystalline DMPC membranes. In contrast, the hydrophobic transmembrane peptide WALP23 undergoes vigorous fluctuations, and here our data analysis clearly shows that dynamics must not be ignored; otherwise, the calculated helix tilt angles are underestimated.

In previous ^{2}H-NMR studies of WALP23 and related peptides, the helix tilt in different lipid systems had been found to be very small and only weakly dependent on hydrophobic mismatch (3,7,9,13). These reports were not supported by the results from more recent MD simulations, which systematically showed larger peptide tilts that were also much more influenced by bilayer mismatch (21,22). Our dynamic analysis also yields a larger tilt for WALP23 in DMPC and DLPC than previously published, although the tilts from the simulations are still larger than these new experimental values (21–23). On the other hand, the observed difference between the two lipid systems appears now in better agreement with the hydrophobic mismatch predictions. To obtain yet another independent picture for this kind of mobile transmembrane peptide, an alternative method such as two-dimensional NMR PISEMA should be applied, as it has been suggested that rigid-body peptide dynamics would have only a small influence on the analysis of polar index slant angles (PISA) wheels in ^{15}N PISEMA spectra (43). A use of both ^{2}H-NMR on Ala-d_3 labels and ^{15}N PISEMA spectra has been reported recently to study the model membrane peptide GWALP23, which is similar to WALP23, and basically the same tilt has been obtained from the two methods using static models to analyze the data (15). However, this might be a particular case with low peptide mobility. In the accompanying article we have investigated the effects of dynamics in PISEMA spectra for a wide range of cases (25), with the conclusion that the PISEMA analysis of a highly mobile transmembrane peptide is indeed less model dependent, yet it can yield the same valuable insights on helix wagging and rotational oscillations as ^{2}H-NMR.

SUPPORTING MATERIAL

Analysis, comments, evaluation, six figures, and two tables are available at http://www.biophysj.org/biophysj/supplemental/S0006-3495(09)00602-X.

We thank the DFG-Center for Functional Nanostructures in Karlsruhe for financing of the NMR infrastructure (E1.2). This work has been supported by a grant from the Spanish Ministerio de Educación y Ciencia, MEC (BFU200767097), which is financed in part by the European Regional Development Fund (ERDF). S.E. thanks MEC for an Formacion de Personal Investigador (FPU) fellowship and the European Molecular Biology Organization for a short-term fellowship.

REFERENCES

1. Strandberg, E., and A. S. Ulrich. 2004. NMR methods for studying membrane-active antimicrobial peptides. *Concepts Magn. Reson. A.* 23A:89–120.
2. Ulrich, A. S. 2005. Solid state ^{19}F-NMR methods for studying biomembranes. *Prog. Nucl. Magn. Reson. Spectrosc.* 46:1–21.
3. Van der Wel, P. C. A., E. Strandberg, J. A. Killian, and R. E. Koeppe, 2nd. 2002. Geometry and intrinsic tilt of a tryptophan-anchored transmembrane α-helix determined by ^{2}H NMR. *Biophys. J.* 83: 1479–1488.
4. Afonin, S., U. H. N. Dürr, R. W. Glaser, and A. S. Ulrich. 2004. 'Boomerang'-like insertion of a fusogenic peptide in a lipid membrane revealed by solid-state ^{19}F NMR. *Magn. Reson. Chem.* 42:195–203.
5. Glaser, R. W., C. Sachse, U. H. Dürr, P. Wadhwani, and A. S. Ulrich. 2004. Orientation of the antimicrobial peptide PGLa in lipid membranes determined from ^{19}F-NMR dipolar couplings of 4-CF_3-phenylglycine labels. *J. Magn. Reson.* 168:153–163.
6. Ramamoorthy, A., Y. F. Wei, and D. K. Lee. 2004. PISEMA solid-state NMR spectroscopy. *Adv. Solid State NMR Stud. Mater. Polymers. A Special Volume Dedicated to Isao Ando.* 52:1–52.
7. Strandberg, E., S. Özdirekcan, D. T. S. Rijkers, P. C. A. Van der Wel, R. E. Koeppe, 2nd, et al. 2004. Tilt angles of transmembrane model peptides in oriented and non-oriented lipid bilayers as determined by ^{2}H solid state NMR. *Biophys. J.* 86:3709–3721.
8. Glaser, R. W., C. Sachse, U. H. N. Dürr, S. Afonin, P. Wadhwani, et al. 2005. Concentration-dependent realignment of the antimicrobial peptide PGLa in lipid membranes observed by solid-state ^{19}F-NMR. *Biophys. J.* 88:3392–3397.
9. Özdirekcan, S., D. T. Rijkers, R. M. Liskamp, and J. A. Killian. 2005. Influence of flanking residues on tilt and rotation angles of transmembrane peptides in lipid bilayers. A solid-state ^{2}H NMR study. *Biochemistry.* 44:1004–1012.
10. Strandberg, E., P. Wadhwani, P. Tremouilhac, U. H. N. Dürr, and A. S. Ulrich. 2006. Solid-state NMR analysis of the PGLa peptide orientation in DMPC bilayers: structural fidelity of ^{2}H-labels versus high sensitivity of ^{19}F-NMR. *Biophys. J.* 90:1676–1686.
11. Tremouilhac, P., E. Strandberg, P. Wadhwani, and A. S. Ulrich. 2006. Conditions affecting the re-alignment of the antimicrobial peptide PGLa

in membranes as monitored by solid state ^{2}H-NMR. *Biochim. Biophys. Acta*. 1758:1330–1342.

12. Tremouilhac, P., E. Strandberg, P. Wadhwani, and A. S. Ulrich. 2006. Synergistic transmembrane alignment of the antimicrobial heterodimer PGLa/magainin. *J. Biol. Chem.* 281:32089–32094.
13. Daily, A. E., D. V. Greathouse, P. C. van der Wel, and R. E. Koeppe 2nd. 2008. Helical distortion in tryptophan- and lysine-anchored membrane-spanning α-helices as a function of hydrophobic mismatch: a solid-state deuterium NMR investigation using the geometric analysis of labeled alanines method. *Biophys. J.* 94:480–491.
14. Strandberg, E., N. Kanithasen, D. Tiltak, J. Bürck, P. Wadhwani, et al. 2008. Solid-State NMR analysis comparing the designer-made antibiotic MSI-103 with its parent peptide PGLa in lipid bilayers. *Biochemistry*. 47:2601–2616.
15. Vostrikov, V. V., C. V. Grant, A. E. Daily, S. J. Opella, and R. E. Koeppe 2nd. 2008. Comparison of ''Polarization Inversion with Spin Exchange at Magic Angle'' and ''Geometric Analysis of Labeled Alanines'' methods for transmembrane helix alignment. *J. Am. Chem. Soc.* 130:12584–12585.
16. Huang, H. W. 2000. Action of antimicrobial peptides: two-state model. *Biochemistry*. 39:8347–8352.
17. Huang, H. W. 2006. Molecular mechanism of antimicrobial peptides: the origin of cooperativity. *Biochim. Biophys. Acta*. 1758:1292–1302.
18. Axelsen, P. H., B. K. Kaufman, R. N. McElhaney, and R. N. Lewis. 1995. The infrared dichroism of transmembrane helical polypeptides. *Biophys. J.* 69:2770–2781.
19. Prosser, R. S., and J. H. Davis. 1994. Dynamics of an integral membrane peptide: a deuterium NMR relaxation study of gramicidin. *Biophys. J.* 66:1429–1440.
20. Davis, J. H., M. Auger, and R. S. Hodges. 1995. High resolution ^{1}H nuclear magnetic resonance of a transmembrane peptide. *Biophys. J.* 69:1917–1932.
21. Esteban-Martin, S., and J. Salgado. 2007. The dynamic orientation of membrane-bound peptides: bridging simulations and experiments. *Biophys. J.* 93:4278–4288.
22. Özdirekcan, S., C. Etchebest, J. A. Killian, and P. F. Fuchs. 2007. On the orientation of a designed transmembrane peptide: toward the right tilt angle? *J. Am. Chem. Soc.* 129:15174–15181.
23. Kandasamy, S. K., and R. G. Larson. 2006. Molecular dynamics simulations of model trans-membrane peptides in lipid bilayers: a systematic investigation of hydrophobic mismatch. *Biophys. J.* 90:2326–2343.
24. Marrink, S. J., H. J. Risselada, S. Yefimov, D. P. Tieleman, and A. H. de Vries. 2007. The MARTINI force field: Coarse grained model for biomolecular simulations. *J. Phys. Chem. B*. 111:7812–7824.
25. Esteban-Martín, S., E. Strandberg, G. Fuertes, A. S. Ulrich, and J. Salgado. 2009. Influence of whole-body dynamics on ^{15}N PISEMA NMR spectra of membrane peptides: a theoretical analysis. *Biophys. J.* 96:3233–3241.
26. Killian, J. A., I. Salemink, M. R. de Planque, G. Lindblom, R. E. Koeppe, 2nd, et al. 1996. Induction of nonbilayer structures in diacylphosphatidylcholine model membranes by transmembrane alpha-helical peptides: importance of hydrophobic mismatch and proposed role of tryptophans. *Biochemistry*. 35:1037–1045.
27. Afonin, S., P. K. Mikhailiuk, I. V. Komarov, and A. S. Ulrich. 2007. Evaluating the amino acid CF_3-bicyclopentylglycine as a new label for solid-state ^{19}F-NMR structure analysis of membrane-bound peptides. *J. Pept. Sci.* 13:614–623.
28. Wadhwani, P., J. Bürck, E. Strandberg, C. Mink, S. Afonin, et al. 2008. Using a sterically restrictive amino acid as a ^{19}F-NMR label to monitor and control peptide aggregation in membranes. *J. Am. Chem. Soc.* 130:16515–16517.
29. Matsuzaki, K. 1998. Magainins as paradigm for the mode of action of pore forming polypeptides. *Biochim. Biophys. Acta*. 1376:391–400.
30. Oren, Z., and Y. Shai. 1998. Mode of action of linear amphipathic α-helical antimicrobial peptides. *Biopolymers*. 47:451–463.
31. Davis, J. H. 1983. The description of membrane lipid conformation, order and dynamics by ^{2}H-NMR. *Biochim. Biophys. Acta*. 737:117–171.
32. Killian, J. A., and T. K. Nyholm. 2006. Peptides in lipid bilayers: the power of simple models. *Curr. Opin. Struct. Biol.* 16:473–479.
33. Petrache, H. I., D. M. Zuckerman, J. N. Sachs, J. A. Killian, R. E. Koeppe, et al. 2002. Hydrophobic matching mechanism investigated by molecular dynamics simulations. *Langmuir*. 18:1340–1351.
34. Goodyear, D. J., S. Sharpe, C. W. Grant, and M. R. Morrow. 2005. Molecular dynamics simulation of transmembrane polypeptide orientational fluctuations. *Biophys. J.* 88:105–117.
35. Im, W., and C. L. Brooks, 3rd. 2005. Interfacial folding and membrane insertion of designed peptides studied by molecular dynamics simulations. *Proc. Natl. Acad. Sci. USA*. 102:6771–6776.
36. Nymeyer, H., T. B. Woolf, and A. E. Garcia. 2005. Folding is not required for bilayer insertion: replica exchange simulations of an alpha-helical peptide with an explicit lipid bilayer. *Proteins*. 59:783–790.
37. Bond, P. J., J. Holyoake, A. Ivetac, S. Khalid, and M. S. Sansom. 2007. Coarse-grained molecular dynamics simulations of membrane proteins and peptides. *J. Struct. Biol.* 157:593–605.
38. Davis, J. H., K. R. Jeffrey, M. Bloom, M. I. Valic, and T. P. Higgs. 1976. Quadrupolar echo deuteron magnetic resonance spectroscopy in ordered hydrocarbon chains. *Chem. Phys. Lett.* 42:390–394.
39. Salgado, J. B., S. L. Grage, L. H. Kondejewski, R. N. McElhaney, R. S. Hodges, et al. 2001. Alignment of the antimicrobial β-sheet peptide gramicidin S in membranes: a solid state ^{19}F-NMR study in oriented lipid bilayers. *J. Biomol. NMR*. 21:191–208.
40. Kim, S., and T. A. Cross. 2002. Uniformity, ideality, and hydrogen bonds in transmembrane alpha-helices. *Biophys. J.* 83:2084–2095.
41. Page, R. C., S. Kim, and T. A. Cross. 2008. Transmembrane helix uniformity examined by spectral mapping of torsion angles. *Structure*. 16:787–797.
42. Page, R. C., C. Li, J. Hu, F. P. Gao, and T. A. Cross. 2007. Lipid bilayers: an essential environment for the understanding of membrane proteins. *Magn. Reson. Chem.* 45:S2–S11.
43. Straus, S. K., W. R. P. Scott, and A. Watts. 2003. Assessing the effects of time and spatial averaging in ^{15}N chemical shift/^{15}N-^{1}H dipolar correlation solid state NMR experiments. *J. Biomol. NMR*. 26:283–295.